Energetics and spin and Λdoublet selectivity in the infrared multiphoton dissociation HN3(X̃1 A')→N2(X 1Σ+ g)+NH(X 3Σ−,a 1Δ): Theory

Millard H. Alexander, HansJoachim Werner, and Paul J. Dagdigian

Citation: The Journal of Chemical Physics **89**, 1388 (1988); doi: 10.1063/1.455138
View online: http://dx.doi.org/10.1063/1.455138
View Table of Contents: http://scitation.aip.org/content/aip/journal/jcp/89/3?ver=pdfcov
Published by the AIP Publishing

Energetics and spin- and Λ-doublet selectivity in the infrared multiphoton dissociation $HN_3(\tilde{X}\,^1A') \rightarrow N_2(X\,^1\Sigma_g^+) + NH(X\,^3\Sigma^-, a\,^1\Delta)$: Theory

Millard H. Alexander
Department of Chemistry, University of Maryland, College Park, Maryland 20742

Hans-Joachim Werner
Fakultät für Chemie der Universität Bielefeld, D-4800 Bielefeld, West Germany

Paul J. Dagdigian
Department of Chemistry, The Johns Hopkins University, Baltimore, Maryland 21218

(Received 15 March 1988, accepted 1 April 1988)

An investigation of the energetics and mechanism of the dissociation of ground state $HN_3(\tilde{X}\,^1A')$ into ground state $N_2(X\,^1\Sigma_g^+) + NH(X\,^3\Sigma^-)$ products is presented. This process, which can be induced by multiphoton infrared pumping, occurs through a crossing between the lowest-energy singlet potential energy, which correlates asymptotically with electronically excited NH products ($a\,^1\Delta$), and the lowest triplet surface. By means of *ab initio* CASSCF and MCSCF-CI calculations we have determined that the geometry at the minimum singlet–triplet crossing corresponds to an approximately linear N_3 backbone with a perpendicular NH bond. The interior N–N distance is $\sim$3.6 bohr. This transition state lies $\sim$12 500 cm^{-1} above the energy of $\tilde{X}\,^1A'$ state of HN_3 at the experimental equilibrium geometry. Since the N–N and N–H bonds are perpendicular at this transition state, there will be no torques tending to twist the system out of a planar geometry. The crucial singlet–triplet coupling occurs because the HN_3 wave function in the region of this transition state can be considered an equal admixture of $N_2(X)\cdot NH(a\,^1\Delta)$ and $N_2(X)\cdot NH(b\,^1\Sigma^+)$. Since the ground state HN_3 wave function as well as the relevant spin–orbit Hamiltonian are symmetric with respect to reflection of the spatial and spin components of all the electrons in the plane of the molecule, and since the NH fragment must rotate in the plane of the initital HN_3 molecule if the dissociation is planar, NH products can be formed only in states in which the wave function (electronic + rotational) is also symmetric with respect to this operation. For a molecule in a $^3\Sigma^-$ electronic state the wave functions in only the F_1 and F_3 multiplets will be symmetric so that one would expect population in only the F_1 and F_3 levels. A similar symmetry argument implies that the NH products formed in the lowest spin-allowed channel $[N_2(X\,^1\Sigma_g^+) + NH(a\,^1\Delta)]$ will be found predominantly in the $\Delta(A')$ Λ-doublet state, which is symmetric with respect to reflection of the spatial coordinates of the electrons in the plane of rotation. This spin- and Λ-doublet selectivity has been found experimentally by Stephenson, Casassa, and King (accompanying article). The implications of similar spin selectivity in other photodissociation processes leading to molecules in $^3\Sigma^-$ states, e.g., $SO(X\,^3\Sigma^-)$ and $O_2(X\,^3\Sigma_g^-)$, are also considered.

I. INTRODUCTION

In many photodissociation reactions one or more of the diatomic fragments are formed in open-shell electronic states. The distribution of the products among the various possible fine-structure levels can, in principle, provide considerable insight into the photolytic mechanism. Much attention has been focused on fragments in $^2\Pi$ electronic states, where the rotational ladder is split into two spin–orbit manifolds and each rotational level is further split into a closely spaced Λ doublet, which correspond to linear combinations of the $+\Lambda$ and $-\Lambda$ projections of the electronic orbital angular momentum.[1] For sufficiently high angular momentum J, these two levels have opposite symmetry with respect to reflection through the plane of rotation.[2,3] The nonstatistical population of upper or lower Λ-doublet levels of product molecules in $^2\Pi$ electronic states has been reported in a number of photodissociation processes producing either $OH(X\,^2\Pi)$,[4–7] $NO(X\,^2\Pi)$,[8–10] or $NH(c\,^1\Pi)$.[11,12] In many of these studies, the preferential production of a given Λ-doublet level has been interpreted by analysis of the evolution of the molecular orbitals of the precursor species which correlate with the unfilled π molecular orbital in the diatomic fragment.

A similarly simple explanation is unfortunately not available for unequal populations in the two spin–orbit manifolds of NO, which have been observed in a number of photodissociation processes.[8,10,13–16] Recently Wittig and Zare and their co-workers[17,18] have observed nonstatistical populations in the spin–doublet levels of the CN molecule in its ground $X\,^2\Sigma^+$ electronic state produced by photolysis of ICN. In principle, it might be easier to understand spin selectivity in photodissociation leading to a molecule in a $^{2S+1}\Sigma$ state, rather than a $^{2S+1}\Pi$ state, since any complications arising from the presence of a nonzero orbital electronic orbital angular momentum are absent. In a molecule in a

 0021-9606/88/151388-13$02.10

$^{2S+1}\Sigma$ electronic state the $(2S+1)$ spin multiplets correspond to the allowed vector coupling of the spin (S) and nuclear rotational (N) angular momentum.[1] The origin of spin selectivity must be qualitatively different than that of the Λ doublet specificity discussed in the first paragraph, since in the former case the selectivity corresponds to a preferential orientation of the electron *spin* relative to some internal axis, rather than a preferential *spatial* orientation of the electronic wave function.[2,3] In the case of the ICN photodissociation, an interesting explanation has been given by Joswig, O'Halloran, Zare, and Child[18] in terms of out-of-plane forces resulting from the coupling of the total angular momentum of the receding halogen atom with the nuclear rotational angular momentum of the CN molecule.

Preferential population of spin levels in photodissociation products formed in $^3\Sigma$ electronic states has also been found. Recently, Stephenson, Casassa, and King[19] (accompanying article) have observed an intriguing spin selectivity in the dissociation of deuterated hydrazoic acid (DN_3) to form ground state ND molecules:

$$DN_3(\tilde{X}\,^1A') \xrightarrow{nh\nu} ND(X\,^3\Sigma^-) + N_2(X\,^1\Sigma_g^+)\,. \qquad (1)$$

This dissociation is induced by infrared multiphoton pumping and therefore takes place on the ground electronic surface. An even stronger spin selectivity has been seen by Foy, Casassa, Stephenson, and King[20] in the dissociation of HN_3 by single-photon overtone pumping. As written, process (1) is spin forbidden; the spin-allowed pathway would lead to the lowest electronically excited product channel of singlet multiplicty, which correlates with the ND fragment in its lowest singlet state ($a\,^1\Delta$). Formation of $ND(a\,^1\Delta)$ is in fact observed both in the multiphoton experiments of Stephenson, Casassa, and King,[19] and in the ultraviolet photodissociation of hydrazoic acid.[21–23]

Decomposition according to Eq. (1) must occur by a spin–orbit induced crossing between the singlet surface correlating asymptotically to $N_2(X\,^1\Sigma_g^+) + ND(a\,^1\Delta)$ and the lowest triplet surface, which correlates asymptotically with the ground state product channel $[N_2(X\,^1\Sigma_g^+) + ND(X\,^3\Sigma^-)]$. The latter, however, correlates in the molecular region with an electronically excited triplet state of DN_3. This is illustrated schematically in Fig. 1. Experimentally, production of $ND(X\,^3\Sigma^-)$ is monitored by laser-induced fluorescence.[19,20] The ND molecule is found to be produced preferentially in the F_1 and F_3 spin multiplet levels, with little population in the F_2 levels.

Three factors are essential to an understanding of the dynamics of the dissociation of hydrazoic acid studied by Stephenson, Casassa, Foy, and King.[19,20] The first is the location of the crossing between the lowest singlet and lowest triplet surfaces (Fig. 1). The height of the barrier will determine the ease with which spin-forbidden products can be obtained by infrared multiphoton pumping. In addition the location of the barrier, and the gradient of the triplet surface after the barrier, will determine the degree to which the internal energy of the HN_3 molecule is transformed into internal or translational energy of the fragments. The second crucial factor is the origin of the singlet–triplet coupling which leads to the formation of triplet NH from a singlet state of

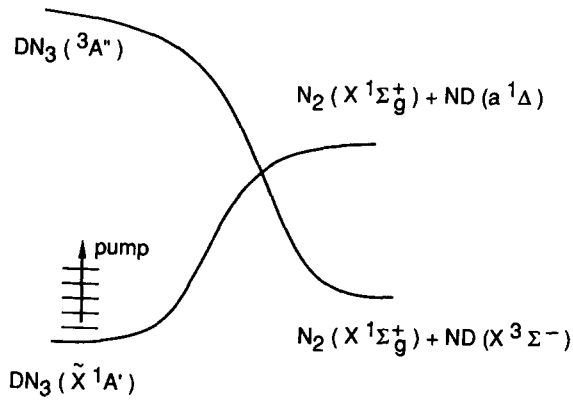

FIG. 1. Schematic reaction coordinate diagram for the energetics of the dissociation of DN_3 by multiphoton pumping on the ground electronic surface.

HN_3. As discussed above, the lowest spin-allowed channel is $N_2(X\,^1\Sigma_g^+) + NH(a\,^1\Delta)$, and the lowest triplet channel is $N_2(X\,^1\Sigma_g^+) + NH(X\,^3\Sigma^-)$. At first glance the singlet–triplet coupling would thus appear to arise from spin–orbit mixing in the NH molecule as it separates from the N_2 fragment. However, it is well-known that for the isolated NH molecule the spin–orbit Hamiltonian will *not* couple $^1\Delta$ and $^3\Sigma^-$ electronic states.[24] Third, it is important to understand the startling spin-state selectivity. As will be shown, in the case of the formation of $NH(X\,^3\Sigma^-)$ from hydrazoic acid, this spin selectivity can be understood in terms of the symmetry of the initial (singlet) and final (triplet) wave functions, provided that the crucial singlet–triplet coupling occurs for a planar HN_3 geometry. As will be discussed below, the term in the spin–orbit Hamiltonian which causes the mixing between the initial $\tilde{X}\,^1A'$ state of HN_3 and the dissociative triplet state, which correlates with $N_2(X\,^1\Sigma_g^+) + NH(X\,^3\Sigma^-)$ products, is symmetric with respect to reflection in the plane of the molecule. Thus the initial symmetric electronic state will only be mixed only with triplet states which are similarly symmetric. As will be shown, since the F_1 and F_3 spin–triplet levels are symmetric and the F_2 levels, antisymmetric, production of the F_2 levels will be forbidden.

A similar nonstatistical spin-state distribution has been found by Kanamori *et al.*[25] in the 193 nm photodissociation of sulfur dioxide, namely,

$$SO_2(\tilde{X}\,^1A_1) \xrightarrow{h\nu} SO(X\,^3\Sigma^-) + O(^3P)\,. \qquad (2)$$

The internal state distribution of the $SO(X\,^3\Sigma^-)$ product is monitored by transient infrared absorption spectroscopy. This photodissociation process is ascribed[25] to initial excitation of the $SO_2(\tilde{C}\,^1B_2)$ electronic state, which correlates asymptotically to $SO(a\,^1\Delta) + O(^1D)$ products. Formation of ground-state SO is believed to occur by spin–orbit induced transitions to a repulsive $^3A'$ surface which correlates at large SO–O distances to the ground-state product channel $[SO(X\,^3\Sigma^-) + O(^3P)]$. For SO molecules formed in the $v=1$ and $v=2$ vibrational levels a strong preference was seen for population of the F_1 and F_3 levels. This selective

population was not observed for the $v = 5$ level, whose population is considerably less than for the lower vibrational levels.

In the next section of this article we report the results of *ab initio* calculations on the HN_3 molecule undertaken to determine the location and height of the singlet–triplet crossing. As will be discussed in Sec. III, an analysis of the HN_3 wave functions for the lowest singlet state in the region of this singlet–triplet crossing can easily explain the facility of the spin-forbidden dissociation observed by Stephenson, Casassa, Foy, and King.[19,20] The origin of the spin-state selectivity, which we ascribed to the overall symmetry of the initial and final wave functions, will be discussed in detail in Sec. IV. In addition, in Sec. V we discuss how an identical symmetry argument predicts that NH products formed in the lowest spin-allowed (singlet) channel,

$$HN_3(\tilde{X}\,^1A') \rightarrow NH(a\,^1\Delta) + N_2(X\,^1\Sigma_g^+)\,, \qquad (3)$$

will be found preferentially in the $\Delta(A')$ Λ-doublet state which is symmetric with respect to reflection of the spatial coordinates of the electrons in the plane of rotation.[3] The article is closed by a short discussion in which we make some predictions about spin selectivity which might be expected in the dissociation of similar molecules.

II. *AB INITIO* STUDIES OF THE SINGLET–TRIPLET TRANSITION STATE FOR HN_3

In its ground ($\tilde{X}\,^1A'$) electronic state the HN_3 molecule is planar with a nearly linear N_3 moiety and the H–N bond strongly bent with respect to the N_3 backbone (see Fig. 2).[26] The wave function can be written in a single-configuration approximation as $1a'^2 \ldots 9a'^2 1a''^2 2a''^2$.[27,28] Here the $1a'$-$3a'$ molecular orbitals correspond to the innershell N $1s$ orbitals; the $4a'$-$9a'$ orbitals to linear combinations of the atomic s and in-plane N $2p$ orbitals, and the $1a''$ and $2a''$ orbitals, to linear combinations of the out-of-plane N $2p$ orbitals. A number of *ab initio* studies of HN_3 have been reported.[27–30] Most have concentrated on the region of the experimental minimum,[27,29,30] although Lievin, Breulet, and Verhaegen[28] have used SCF-CI calculations to explore the $HN_3 \rightarrow N_2 + NH$ singlet dissociation channel.

To characterize quantitatively the orbitals and energetics of the HN_3 molecule, in particular in the region of the singlet–triplet crossing of relevance to the ground state dissociation channel, it is necessary to use an *ab initio* technique which allows for the orbital distortion and changes in electron occupancies which accompany bond formation and breaking. This can be best done using multiconfiguration self-consistent-field (MCSCF)[31–35] and multireference configuration-interaction (MCSCF-CI)[36–38] techniques. We have carried out MCSCF and complete active space self-consistent-field (CASSCF)[35] calculations for the HN_3 molecule at a number of geometries. The MCSCF wave functions then served as zeroth order approximations for the MCSCF-CI calculations.

A number of calculations were done with an atomic orbital basis which consisted of Huzinaga's[39] 10s,6p basis for N with the addition of one d function with exponent 1.0. The innermost four s functions and three p functions were contracted. For the H atom Huzinaga's 6s set was used with the addition of two p functions with exponents 1.2 and 0.3. The innermost three s functions were contracted. This 10/6/1–6/2 basis consisted of a total of 82 contracted Gaussian-type orbitals. The CASSCF calculations included all configurations built from allocating 14 active electrons within an active space of the $5a'$–$11a'$ and $1a''$–$3a''$ orbitals; this resulted in a total of 2528 configurations for the $^1A'$ state and 3486 configurations for the $^3A''$ state. All configurations which in a canonical orbital basis had weights greater than 0.06 in the final CASSCF wave functions were then included in the configuration list for the MCSCF wave functions. These reference configurations are listed in Table I. In the subsequent MCSCF-CI calculations all single and double excitations with respect to the MCSCF reference wave function were considered. Inclusion of all excitations out of all the valence orbitals, except the $4a'$ orbital, which corresponds to the lowest σ-bonding orbital on $N_2(2\sigma_g)$, gives rise to a total of 124 546 and 125 396 internally contracted[36–38] configurations for the $^1A'$ and $^3A''$ states, respectively.

In addition, calculations were carried out at a more restricted set of geometries using a larger basis set consisting of Huzinaga's[39] 11s, 7p basis for N with the addition of two d

TABLE I. MCSCF reference configurations employed in the MC-CI calculations on HN_3.

	For N_2-NH dissociation	At HN_3 equilibrium
	$^1A'$ state	
1	$\ldots 8a'^2 9a'^2 1a''^2 2a''^2$	$\ldots 8a'^2 9a'^2 1a''^2 2a''^2$
2	$\ldots 8a'^2 9a'^2 2a''^2 3a''^2$	$\ldots 8a'^2 9a'^2 1a''^2 3a''^2$
3	$\ldots 9a'^2 11a'^2 1a''^2 2a''^2$	$\ldots 8a'^2 10a'^2 1a''^2 2a''^2$
4	$\ldots 8a'^2 10a'^2 1a''^2 2a''^2$	$\ldots 8a'^2\,{}^1(9a'10a')1a''^2\,{}^1(2a''3a'')$
5	$\ldots {}^1(8a'11a')9a'^2\,{}^1(1a''3a'')2a''^2$	
	$^3A''$ state	
1	$\ldots 8a'^2 9a'^2 1a''^2\,{}^3(10a'2a'')$	
2	$\ldots 8a'^2 9a'^2 3a''^2\,{}^3(10a'2a'')$	
3	$\ldots 8a'^2 11a'^2 1a''^2\,{}^3(10a'2a'')$	

functions with exponents 1.6 and 0.4. The innermost six s functions and four p functions were contracted. For the H atom Huzinaga's 7s set was used with the addition of two p functions with exponents 1.2 and 0.3. The innermost four s functions were contracted. This 11/7/2–7/2 basis consisted of a total of 94 contracted Gaussian-type orbitals. Here the CI calculations, which again included all single and double excitations out of all valence orbitals, except the 4a' orbital, gave rise to 168 878 and 167 632 internally contracted[36–38] configurations for the $^1A'$ and $^3A''$ states, respectively. The CASSCF calculations with this larger basis set included configurations built from allocating 14 active electrons within an active space of the 5a'–12a' and 1a''–3a'' orbitals; this resulted in a total of 16 542 configurations for the $^1A'$ state and 25 424 configurations for the $^3A''$ state. In comparison with the CASSCF calculations with the smaller 10/6/1–6/2 basis, the active space here was extended to include the 12a orbital.

Table II presents a comparison of the results of the present calculation with those of several previous calculations[27–30] of HN_3 at or near the experimental minimum.[26] Since our goal was not to determine the absolute minimum of the HN_3 molecule we carried out calculations only at the experimental minimum[26] and at the minimum found by McLean and co-workers[30] in an SCF + CI calculation. As can be seen, our MCSCF + CI energy lies below the comparable variational value reported by these authors,[30] although they ultimately obtain a lower nonvariational energy by adding the estimate of the contribution of quadruple excitations to the total CI wave function proposed by Langhoff and Davidson.[40] Our CI energies are still lower at the optmized geometry of McLean *et al.*[30] than at the experimental geometry, but with the 11/7/2–7/2 basis the difference between the computed energies at these two geometries is very small.

Another measure of the quality of the basis sets used here is the predicted energy splittings between the $X\,^3\Sigma^-$ and $a\,^1\Delta$ states of the NH molecule and the predicted dipole moments in these states. These are compared in Table III with values from previous calculations by Meyer and Rosmus[41] and Marian and Klotz.[42] In contrast to the case for the HN_3 molecule (Table II), the 10/6/1–6/2 basis yields a slightly more accurate value of the $X\,^3\Sigma^-$–$a\,^1\Delta$ splitting, as well as slightly lower total energies.

Calculations were also carried out at a number of dissociative geometries to find the locus of crossings between the $^1A'$ and $^3A''$ surfaces. Since a four-atom system can be described by six internal coordinates, this locus of crossings is a five-dimensional hypersurface. The minimum on this surface, with respect to the energy of the HN_3 $\tilde{X}\,^1A'$ ground state, will define the height of the barrier for formation of $N_2(X\,^1\Sigma_g^+) + NH(X\,^3\Sigma^-)$ by dissociation on the ground state potential energy surface of HN_3. Initial CASSCF calculations using the 10/6/1–6/2 basis set revealed that this singlet–triplet crossing minimum occurred for a nearly linear N_3 backbone with the N–H bond perpendicular to the N_3

TABLE II. *Ab initio* energies for the ground ($\tilde{X}\,^1A'$) electronic state of HN_3 near its equilibrium geometry.[a]

Method	r_{HN_1}	$r_{N_1N_2}$	$r_{N_2N_3}$	∠(HNN)	∠(NNN)	Energy	Authors
SCF	1.0175	1.2680	1.1085	108.48	172.09	−163.583 218	b
SCF	1.021	1.238	1.132	112.0	175.0	−163.849 4	c
SCF	1.02	1.27	1.125	111	170	−163.729 2	d
SCF + CI	1.02	1.27	1.125	111	170	−163.914 5	d
SCF + CI	1.02	1.27	1.125	111	170	−163.924 7	d
SCF	1.006	1.242	1.098	108.3	174.5	−163.878 21	e
SCF + SDCI	1.015	1.250	1.127	107.8	173.1	−163.322 19	e
SCF + SDCI + Q	1.019	1.257	1.139	107.5	172.4	−163.376 75	e,f
MCSCF + SDCI	1.015	1.250	1.127	107.8	173.1	−163.336 713	g
						−163.360 598	g
MCSCF	1.015	1.243	1.134	108.8	171.3	−163.973 345	g
						−163.982 162	
CASSCF	1.015	1.243	1.134	108.8	171.3	−164.018 696	g
						−164.079 578	
MCSCF + SDCI	1.015	1.243	1.134	108.8	171.3	−164.336 548	g
						−164.360 499	g
Experiment	1.015	1.243	1.134	108.8	171.3		h

[a] Distances in Å, angles in deg, energies in hartree. A planar *trans* $HN_1N_2N_3$ geometry is assumed (Fig. 2).
[b] Reference 27.
[c] Reference 28.
[d] Reference 29.
[e] Reference 30.
[f] Contribution of quadruple excitations estimated by Davidson correction (Ref. 40).
[g] Present calculations. Where two entries are present, the first refers to calculations with a 10/6/1–6/2 basis (see the text) and the second, to a 11/7/2–7/2 basis. In the CASSCF calculations the orbitals were optimized for the lowest $^1A'$ and $^3A''$ states simultaneously (Refs. 32–34) in the 10/6/1–6/2 calculations, but only for lowest $^1A'$ state in the 11/7/2–7/2 calculations. The geometries were not optimized.
[h] Reference 26.

TABLE III. Vertical excitation energies and dipole moments of NH.

Method	T_v (cm^{-1}) $a\,^1\Delta$	μ (D) $X\,^3\Sigma^-$	μ (D) $a\,^1\Delta$
CEPA[a]		1.58	
MRD-CI[b]	14 379	1.61	1.61
	13 990	1.63	1.60
	13 128	1.57	1.54
MCSCF-CI[c]	13 799	1.56	1.54
	14 203	1.54	1.53
Experiment[d]	12 718[e]		1.49 ± 0.06[f]

[a] Reference 41.

[b] Reference 42; the three results correspond to successively larger basis sets (basis sets II, III, and IV of Ref. 42).

[c] Present calculations; the first entry refers to a 10/6/1–6/2 basis (see the text) and the second, to a 11/7/2–7/2 basis. The reference configurations were $1\sigma^2 2\sigma^2 3\sigma^2 1\pi_x 1\pi_y$ and $1\sigma^2 2\sigma^2 4\sigma^2 1\pi_x 1\pi_y$ for the $X\,^3\Sigma^-$ state and $1\sigma^2 2\sigma^2 3\sigma^2(1\pi_x^2 - 1\pi_y^2)$ and $1\sigma^2 2\sigma^2 4\sigma^2(1\pi_x^2 - 1\pi_y^2)$ for the $a\,^1\Delta$ state. For the $a\,^1\Delta$ state $\pi \rightarrow \pi^*$ excitations are more important than for the $X\,^3\Sigma^-$ state. Since these were not included in the reference function for the CI calculations carried out here, the calculated $X\,^3\Sigma^- - a\,^1\Delta$ splitting is slightly too high compared to experiment.

[d] C. R. Brazier, R. S. Ram, and P. F. Bernath (BRB), J. Mol. Spectrosc. **120**, 381 (1986).

[e] The value given is an estimate of T_e, obtained by adding to the experimental value of $T_0(a \leftarrow X)$ of 12 688.39 cm^{-1} (BRB) the difference in the zero-point energies in the $a\,^1\Delta$ and $X\,^3\Sigma^-$ states. These zero-point energies are estimated using values of ω_e and $\omega_e x_e$ calculated from the vibrational term values given in Tables IX and X of BRB. We find, for the $X\,^3\Sigma^-$ state, $\omega_e = 3281.84$ cm^{-1} and $\omega_e x_e = 78.13$ cm^{-1} and, for the $a\,^1\Delta$ state, $\omega_e = 3231.7$ cm^{-1} and $\omega_e x_e = 98.48$ cm^{-1}.

[f] T. A. R. Irwin and F. W. Dalby, Can. J. Phys. **43**, 1766 (1965).

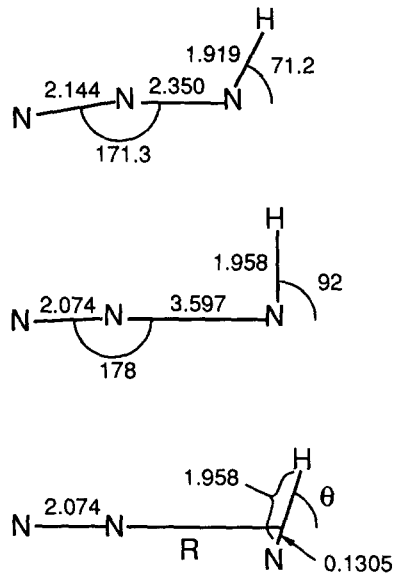

FIG. 2. Geometry of HN_3. The top diagram illustrates the geometry at the experimental minimum for the $\tilde{X}\,^1A'$ state. The middle diagram illustrates the lowest point of crossing between the $^1A'$ and lowest $^3A''$ surface, predicted by the MCSCF-CI calculations with a 10/6/1–6/2 basis. This point corresponds to the curve crossing depicted in Fig. 1. Finally, the bottom diagram illustrates the coordinates used to investigate the torque on the NH fragment during dissociation. The coordinate R designates the distance between the middle N atom and the center-of-mass of the NH molecule, and the angle θ is the relative polar angle between the N–N and N–H bonds. Distances are given in bohr, angles in degrees.

backbone. The terminal N–N bond distance and the N–H bond distance were very close to the equilibrium internuclear separations in the ground electronic states of these two molecules [2.074 bohr for $N_2(X\,^1\Sigma_g^+)$ and 1.958 bohr for $NH(X\,^3\Sigma^-)$[43]], and the interior N–N distance was approximately 3.5 bohr. Although it was not possible to carry out a complete search of the six dimensional space at the CI level, a series of MCSCF-CI calculations with the 10/6/1–6/2 basis revealed that the singlet–triplet crossing minimum lies at (or close to) the geometry shown in Fig. 2. At this point the singlet–triplet crossing lies 12 902 cm^{-1} (5.879×10^{-2} hartree) above the calculated energy of $HN_3(\tilde{X}\,^1A')$ at the experimental equilibrium geometry (Table II). This calculated barrier height refers to the bottom of the HN_3 well.

As discussed above, a less complete exploration of the locus of singlet–triplet crossings was done with the 11/7/2–7/2 basis. The interior N–N distance was varied while the NNN and NNH angles were constrained to be 175° and 90°, respectively, and the terminal N–N and N–H distances were kept at 2.074 and 1.958 bohr, respectively. The CASSCF and MCSCF-CI calculations predict the singlet–triplet crossing to occur at an interior N–N distance of 3.52 bohr (CASSCF) and 3.62 bohr (MCSCF-CI) and lie 13 500 cm^{-1} (CASSCF) and 12 300 cm^{-1} (MCSCF-CI) above the calculated energy of $HN_3(\tilde{X}\,^1A')$ at the experimental geometry. These values agree quite well with the predictions of the calculations using the smaller 10/6/1–6/2 basis.

Our calculations agree well with the results of the extensive calculations of Lieven *et al.*[28] using a much smaller basis set. These authors found that as the HN_3 molecule dissociated on the lowest singlet surface, leading to $N_2(X\,^1\Sigma_g^+) + NH(a\,^1\Delta)$, the N_2 and NH bond distances rapidly relaxed to the values appropriate to the isolated molecules and the NNH angle decreased to 90°. Their estimate of the height of the singlet–triplet crossing point (~30 kcal/mol = 10 500 cm^{-1}) is, however, considerably lower than our calculated values.

The product internal energy distributions of the fragment N_2 and NH molecules produced by the singlet–triplet crossing during the $HN_3 \rightarrow N_2(X\,^1\Sigma_g^+) + NH(X\,^3\Sigma^-)$ dissociation will be sensitive to the forces exerted on the nascent products as the system crosses over from the $^1A'$ to the $^3A''$ surface. Since, as far as we could ascertain, the bond distances of the N_2 and NH fragments at the position of lowest singlet–triplet crossing are identical to those in the isolated N_2 and NH molecules, and, further, since the bond distances in the three valence states of NH are virtually identical ($r_e = 1.036$ Å in the $X\,^3\Sigma^-$ and $b\,^1\Sigma^+$ states and 1.034 Å in the $a\,^1\Delta$ state[43]), we anticipate that the dissociation process will be vibrationally adiabatic. Since the NNH angle at the point of lowest singlet–triplet crossing is somewhat less than at the equilibrium geometry of HN_3 (~90° as compared to ~110°), one might anticipate some degree of rotational excitation of the NH fragment.

To investigate the torque on the NH fragment as the products dissociate we carried out a series of CASSCF calcu-

lations with the 10/6/1–6/2 basis, varying both the distance between the interior N atom and the center of mass of the NH molecule and the polar angle between the N–N and N–H bonds (see Fig. 2). At each value of the NN–NH distance we determined the polar angles for which the energy of the lowest $^1A'$ and lowest $^3A''$ surfaces was minimum (θ_{min}), as well as the second derivative of the energy with respect to the polar angle at this minimum. In other words we determined both the slope (in terms of the separation coordinate R) and the curvature (in terms of the polar coordinate θ) of the exit canyons in both the $^1A'$ and $^3A''$ surfaces. The results are given in Table IV. Although the 10/6/1–6/2 CASSCF calculations predict a lower singlet–triplet crossing than the calculations with the larger 11/7/2–7/2 basis, we believe that the predicted torques given in Table IV will be reasonably accurate.

We observe first that near the point of crossing the polar angles of the minima are very similar on both surfaces. Thus, from a classical point of view, when the system hops from the $^1A'$ to the $^3A''$ surface, there will be little momentum transfer into the polar degree of freedom. Further, since θ_{min} varies insignificantly with R in the $^3A''$ exit channel, we conclude that the polar torques will be small in the exit channel. Finally, we see that although the $^3A''$ exit channel is steeply repulsive in the separation coordinate R, the curvature in θ is small. This implies that the energy release will be mainly translational, with little rotational excitation of the NH or N_2 fragments.

At equilibrium the HN_3 molecule in the ground ($\tilde{X}\,^1A'$) electronic state is known to be planar.[26] An important question is to ascertain whether this planarity persists during the dissociation process involving the lowest singlet–triplet crossing. *Ab initio* calculations at nonplanar geometries would have been considerably more expensive than those for planar geometries, and consequently were not done. Nevertheless, we believe that the planarity of the molecule will persist during the dissociation process, since at the point of lowest singlet–triplet crossing the terminal N–N bond and the N–H bonds are nearly perpendicular. For an exactly perpendicular geometry the energy will be *independent* of the dihedral angle between the terminal N–N and the N–H bonds. Thus, if the NN···NH system is planar at the point of lowest singlet–triplet crossing, there will be no torques exerted on the fragments causing a loss of planarity.

III. ORIGIN OF THE SINGLET–TRIPLET MIXING IN THE DISSOCIATION OF HN_3

Ab initio calculations can be used not only to investigate the energetics of the HN_3 dissociation, but also to unravel the mechanism whereby facile singlet–triplet transfer occurs, even though in the isolated NH molecule there exists no spin–orbit coupling between the lowest triplet ($X\,^3\Sigma^-$) and lowest singlet ($a\,^1\Delta$) electronic states.

As the N–N···N–H distance becomes large, the molecular orbitals become associated with either the N_2 or NH fragment, as described in Table V. In a single configuration description the lowest energy asymptote $[N_2(X\,^1\Sigma_g^+) + NH(X\,^3\Sigma^-)]$ corresponds to the electron occupancy $1a'^2...9a'^2\ 10a'\ 1a''^2\ 2a''$, where the two singly filled orbitals are triplet coupled. The simplest description of the singlet wave functions of A' symmetry (in C_s geometry) which correlate to $N_2(X\,^1\Sigma_g^+)$ and NH in the lower and upper *singlet* valence states ($a\,^1\Delta$ and $b\,^1\Sigma^+$) can be written as linear combinations of the two configurations $1a'^2...9a'^2\ 10a'^2\ 1a''^2$ and $1a'^2...9a'^2\ 1a''^2\ 2a''^2$, namely

$$\Psi(^1\Delta) = 2^{-1/2}[|1a'^2...9a'^2\ 10a'^2\ 1a''^2| - |1a'^2...9a'^2\ 1a''^2\ 2a''^2|] \quad (4a)$$

and

$$\Psi(^1\Sigma^+) = 2^{-1/2}[|1a'^2...9a'^2\ 10a'^2\ 1a''^2| + |1a'^2...9a'^2 1a''^2\ 2a''^2|]\,. \quad (4b)$$

As the N_2–NH distance decreases, the relative weight of the $1a'^2...9a'^2\ 10a'^2\ 1a''^2$ electron occupancy in the lowest HN_3 wave function of $^1A'$ symmetry decreases dramatically with respect to that of the $1a'^2...9a'^2\ 1a''^2\ 2a''^2$ electron occupancy. This is illustrated in Fig. 3, where we plot the square of

TABLE IV. Dependence on NN–NH distance and angle of the energies of the lowest singlet and triplet potential energy surfaces of HN_3 in the region of the crossing between the two surfaces.[a]

	$^1A'$			$^3A''$		
R	θ_{min}[b]	$E(R,\theta_{min})$[c]	$\left(\frac{\partial^2 E}{\partial\theta^2}\right)_{\theta_{min}}$	θ_{min}[b]	$E(R,\theta_{min})$[c]	$\left(\frac{\partial^2 E}{\partial\theta^2}\right)_{\theta_{min}}$
3.0	81.5	4438	15.57	92.57	28 155	12.45
3.5	88.5	7644	13.37	93.4	7 618	8.55
4.0	92.0	7788	7.05	96.4	− 1 737	4.80

[a] Distances in bohr, angles in deg, and energies in cm^{-1}; values from CASSCF calculations with 10/6/1–6/2 basis set and with the orbitals optimized for the *two* lowest $^1A'$ surface and the lowest $^3A''$ surface simultaneously. For a description of the geometry see Fig. 2.

[b] The quantity θ_{min} is the angle at which the potential energy is lowest, for a fixed value of R.

[c] Values of the energies are given relative to the energy of the $^1A'$ state at the experimental equilibrium (Table II).

TABLE V. Description of N_3H orbitals at large $N_2\cdots NH$ distances.

Orbital	Description
$1a'$–$3a'$	1s N orbital
$4a'$	σ_g orbital on N_2
$5a'$	2s orbital on N of NH
$6a'$	σ_g orbital on N_2
$7a'$	σ_u orbital on N_2
$8a'$	π_u (a') orbital on N_2
$9a'$	NH σ bonding orbital
$10a'$	2p(a') orbital on N atom of NH
$11a'$	π_g (a') orbital on N_2
$1a''$	π_u (a'') orbital on N_2
$2a''$	2p(a'') orbital on N atom of NH
$3a''$	π_g (a'') orbital on N_2

the coefficients of these two configurations in the 10/6/1–6/2 CASSCF wave function.

Thus, as implied by Lievin *et al.*,[28] in the region of moderate N_2–NH distances, the wave function of the ground state ($\tilde{X}\,^1A'$–$1a'^2...9a'^2\ 1a''^2\ 2a''^2$) can be considered, to a first approximation, to be a linear combination of $N_2(X)\cdot NH(a\,^1\Delta)$ and $N_2(X)\cdot NH(b\,^1\Sigma^+)$, that is

$$\Psi(1\,^1A') \cong 2^{-1/2}[\Psi(^1\Delta) + \Psi(^1\Sigma^+)]\,. \tag{5}$$

At moderate distances, the wave function for the lowest $^3A''$ state can be written in a single-configuration description as $1a'^2...9a'^2\ 10a'1a''^2\ 2a''$, which corresponds qualitatively to $N_2(X)\cdot NH(X\,^3\Sigma^-)$. Consequently, the matrix element of the spin–orbit Hamiltonian which couples the $1\,^1A'$ and $1\,^3A''$ electronic wave functions can be expressed qualitatively as

$$\langle\Psi(1\,^1A')|H_{so}|\Psi(1\,^3A'')\rangle \cong 2^{-1/2}[\langle\Psi(^1\Delta)|H_{so}|\Psi(^3\Sigma^-)\rangle + \langle\Psi(^1\Sigma^+)|H_{so}|\Psi(^3\Sigma^-)\rangle]\,. \tag{6}$$

In a diatomic molecule the spin–orbit operator can not couple a $^1\Delta$ state with a $^3\Sigma^-$ state, but *can* couple a $^1\Sigma^+$ state with a $^3\Sigma^-$ state.[24] Specifically, it is the l_zs_z term in the spin–orbit Hamiltonian, where z designates the NH bond axis, which is responsible for this coupling.[24] In the case of NH the recent *ab initio* calculations of Marian and Klotz[42] indicate that the $\langle b\,^1\Sigma^+|H_{so}|X\,^3\Sigma^-\rangle$ matrix element is large ($\sim$65 cm^{-1}). From Eq. (6) we would then predict $\langle\Psi(1\,^1A')|H_{so}|\Psi(1\,^3A'')\rangle \cong 45\ cm^{-1}$.

Thus, to the extent that the HN_3 wave functions in the region of moderate N_2–NH distances can be qualitatively considered as simple products of N_2 and NH wave functions, we see that the spin–orbit matrix element coupling the lowest singlet and lowest triplet HN_3 wave functions can be large, even though these two wave functions correlate asymptotically with $N_2(X) + NH(a\,^1\Delta)$ and $N_2(X) + NH(X\,^3\Sigma^-)$. The substantial coupling arises because in the region of the crossing between the lowest singlet and lowest triplet potential energy surfaces the singlet wave function can be considered to be a product of N_2 with an equal admixture of the $a\,^1\Delta$ and $b\,^1\Sigma^+$ states of NH.

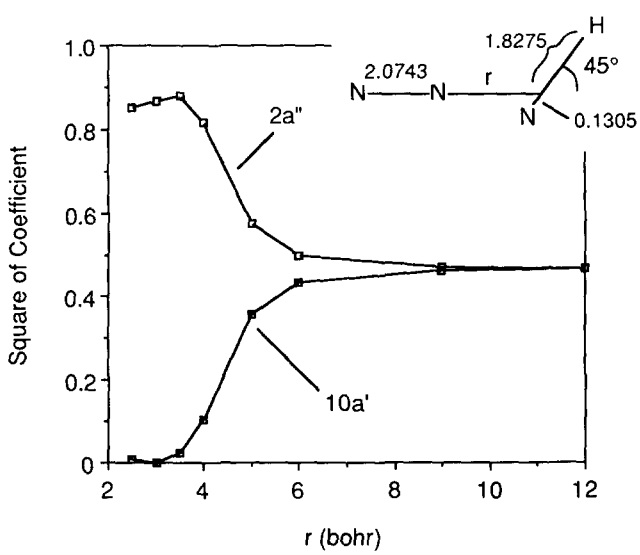

FIG. 3. Squares of the coefficients of the $1a'^2...9a'^2\ 10a'^2\ 1a''^2$ and the $1a'^2...9a'^2\ 1a''^2\ 2a''^2$ configurations in the CASSCF wave functions for the lowest HN_3 state of $^1A'$ symmetry as a function of the distance between the inner N atom and the center-of-mass of the NH molecule. The terminal N–N and NH bond distances are equal to those in the ground electronic states of these two molecules [2.074 bohr for $N_2(X\,^1\Sigma_g^+)$ and 1.958 bohr for $NH(^3\Sigma^-)$]. The other geometrical parameters are illustrated in the figure.

IV. SYMMETRY OF THE ELECTRONIC WAVE FUNCTIONS FOR $^3\Sigma$ ELECTRONIC STATES AND ORIGIN OF THE SPIN SELECTIVITY IN THE DISSOCIATION OF HN_3 TO GIVE $NH(X\,^3\Sigma^-)$ PRODUCTS

As discussed at the end of Sec. II, we anticipate that at the point of lowest singlet–triplet crossing, which is the transition state for the lowest energy dissociation pathway of HN_3, the molecule will be planar, or nearly so. As the N_2 and NH fragments separate, there will be little or no dihedral torques. Thus if no out-of-plane wagging vibrations in the HN_3 molecule are initially excited, then the rotational motion of the nascent NH and N_2 molecules will be confined to the initial HN_3 plane, in other words both the N_2 and NH bond axes will lie in the plane of the initial HN_3 molecule. In the ground state ($\tilde{X}\,^1A'$) the electronic wave function of HN_3 is symmetric with respect to reflection of the spin and space coordinates of the electrons in the molecular plane. Similarly, the l_zs_z term in the spin–orbit Hamiltonian, which, as discussed in Sec. III, is responsible for the coupling between the lowest singlet and lowest triplet surfaces, is symmetric will respect to reflection of the spin and space coordinates of the electrons in any plane containing the NH bond axis—here the HN_3 molecular plane. Since both the initial electronic state, as well as the coupling operator, are symmetric with respect to this operation, coupling will be possible only to final states which are also symmetric.

Since the wave function of the ground state of $N_2(X\,^1\Sigma_g^+)$ is symmetric with respect to reflection of the electronic coordinates in a plane containing the molecular axis, the restriction contained in the last sentence of the preceding paragraph implies that the wave function of the nas-

cent NH molecules in the $X\,^3\Sigma^-$ state must also be symmetric with respect to this operation. As we will see, this restriction will limit population to only two of the possible three spin multiplet levels—those in which the wave function is symmetric with respect to reflection of the electronic coordinates in the plane of the initial HN_3 molecule. At first glance, this might appear paradoxical, since we know that the electronic wave functions of both the lowest triplet states of $HN_3(^3A'')$ and $NH(X\,^3\Sigma^-)$ are *antisymmetric* with respect to reflection. As we will see, however, a proper analysis involves consideration of both the electronic and rotational wave functions of the NH molecule.

The wave functions for molecules in $^3\Sigma$ electronic states are well described in a case (b) or (a) basis depending on whether the phenomenological spin–spin interaction is small or large, respectively.[44,45] This term in the molecular Hamiltonian is the sum of two contributions, the first-order dipolar spin–spin interaction and a second-order spin–orbit term.[46] In the NH $X\,^3\Sigma^-$ state, the former is dominant[47]; however, the symmetry arguments presented below are independent of the exact origin of the phenomenological spin–spin term. We shall first work out the reflection symmetry of the wave functions in the case (a) basis and then show how these results can be transferred to case (b) coupling.

In case (a) coupling, the diatomic molecular wave functions can be expressed as[24,44,45,48,49]

$$|JM\Omega=0\rangle = |JM\Omega\rangle|\Sigma=0\rangle\,, \tag{7}$$

$$|JM\Omega=1,\epsilon\rangle = 2^{-1/2}[|JM\Omega\rangle|\Sigma=+1\rangle + \epsilon|JM,-\Omega\rangle|\Sigma=-1\rangle]\,. \tag{8}$$

Here J denotes the total angular momentum, with projections M and Ω along the space-fixed and molecule-fixed z axes, respectively, and the symmetry index ϵ equals ± 1.[49] For the electronic part of the wave function, Σ represents the projection along the molecule-fixed axis of the total electronic spin ($S=1$). For $^3\Sigma$ states, the electron orbital angular momentum projection Λ equals zero; we have also suppressed the vibrational part of the wave function in Eqs. (7) and (8) for simplicity. The total parity of the $|JM\Omega=0\rangle$ and $|JM\Omega=1,\epsilon\rangle$ wave functions is $(-1)^{J-1+s}$ and $\epsilon(-1)^{J-1+s}$, respectively, where s equals 0 for Σ^+ states and -1 for Σ^- states.[50] These wave functions for $^3\Sigma^-$ electronic states are labeled in modern spectroscopic notation[51] e for $|JM\Omega=0\rangle$ and $|JM\Omega=1,\epsilon=+1\rangle$ and f for $|JM\Omega=1,\epsilon=-1\rangle$; the opposite identification is made for $^3\Sigma^+$ states.

The molecular rotational wave functions in Eqs. (4) and (5) are given by

$$|JM\Omega\rangle = [(2J+1)/4\pi]^{1/2} D^{J*}_{M\Omega}(\alpha\beta,\gamma=0)\,, \tag{9}$$

where $D^J_{M\Omega}$ is a rotation matrix element[52] and $(\alpha\beta\gamma)$ are the Euler angles which specify the orientation of the molecule frame with respect to the space-fixed coordinate system XYZ. Active rotations have been used, as defined by Brink and Satchler.[50,52] The third Euler angle can be chosen arbitrarily for a diatomic molecule, but it must be set consistently for the rotational and electronic parts of the wave function.[48,49] We have set $\gamma=0$ here and have normalized appropriately in Eq. (9). With this choice of γ, when $\beta=\pi/2$ the molecule-fixed x axis lies along $-Z$.

As in our previous papers on the symmetry of Π electronic states,[2] we consider here reflection symmetry in a plane containing the molecular axis (hereafter denoted as the molecule-frame z axis) as the relevant measure of the symmetry of a wave function. In this case, however, we are interested in the expectation value of the operators $\sigma_v(xz)$ and $\sigma_v(yz)$ corresponding to reflection of the spatial *and* spin coordinates of all the electrons. Inclusion of the spin coordinates is especially relevant in the case (a) limit, where the spins are coupled to the molecular axis. We shall see that the results for case (a) coupling are smoothly transferred to the case (b) limit.

The expectation value for $\sigma_v(pq)$, where $pq=xz$ or yz, can be written for the unsymmetrized case (a) wave functions as

$$\langle JM\Omega'|\langle\Sigma'|\sigma_v(pq)|\Sigma\rangle|JM\Omega\rangle = S_{\Omega'\Omega}(J,M)\langle\Sigma'|\sigma_v(pq)|\Sigma\rangle\,, \tag{10}$$

where $S_{\Omega'\Omega}(J,M)$, which was originally defined by Green and Zare,[53] is given by

$$S_{\Omega'\Omega}(J,M) = \frac{2J+1}{4\pi}\int_0^{2\pi} d\alpha \times \int_0^{\pi} \sin\beta\, d\beta\, D^J_{M\Omega'}(\alpha\beta 0) D^{J*}_{M\Omega}(\alpha\beta 0)\,. \tag{11}$$

For the $\Omega=1$ levels, we find that

$$\langle JM\Omega=1,e/f|\sigma_v(pq)|JM\Omega=1,e/f\rangle = \epsilon S_{1,-1}(J,M)\langle\Sigma'=1|\sigma_v(pq)|\Sigma=-1\rangle\,, \tag{12}$$

while for the $\Omega=0$ level, we have

$$\langle JM\Omega=0|\sigma_v(pq)|JM\Omega=0\rangle = \langle\Sigma'=0|\sigma_v(pq)|\Sigma=0\rangle\,. \tag{13}$$

In deriving Eq. (12), we have made use of the fact that $S_{\Omega\Omega'}(J,M)=S_{\Omega'\Omega}(J,M)$.

Our analysis proceeds similarly as in our previous papers.[2] When J is large, the plane of rotation of the molecule can be identified with the xz and yz molecule-frame planes for $M\cong 0$ and $M\cong J$, respectively.[2,53] The result of reflection of the spatial *and* spin coordinates on the electronic wave function is given by[50]

$$\sigma_v(xz)|S\Sigma\rangle = (-1)^{S-\Sigma+s}|S,-\Sigma\rangle \tag{14}$$

and

$$\sigma_v(yz)|S\Sigma\rangle = (-1)^{S+s}|S,-\Sigma\rangle\,, \tag{15}$$

where s equals 0 and 1 for Σ^+ and Σ^- states, respectively. The reflection symmetry for the spin part of the wave function is worked out in detail in Appendix A for wave functions of doublet and triplet multiplicity.

We shall consider in detail only the $M\cong 0$ case; as shown previously when analyzing Π state wave functions,[2] the derived symmetry for reflection through the plane of rotation is independent of the space-frame projection, as one would expect on physical grounds. For $M\cong 0$, we identify the plane of rotation with the xz plane and use the fact that $S_{1,-1}(J,0)$

equals -1 to obtain the following results for the case (a) basis functions of a $^3\Sigma^-$ electronic state:

$$\langle J,M=0,\Omega=1,e/f|\sigma_v(xz)|J,M=0,\Omega=1,e/f\rangle=\epsilon \tag{16}$$

and

$$\langle J,M=0,\Omega=0|\sigma_v(xz)|J,M=0,\Omega=0\rangle=1\,. \tag{17}$$

Hence, we find that in the case (a) limit for a $^3\Sigma^-$ electronic state, the e levels for both $\Omega=0$ and $\Omega=1$ are *symmetric* with respect to reflection in the plane of rotation, while the $\Omega=1,f$ level is *antisymmetric* with reflection.

The $\Omega=0$ and $\Omega=1,\epsilon=+1$ levels are mixed by the $B\,\mathbf{J}\cdot\mathbf{S}$ term in the molecular Hamiltonian.[24,44,45,48] It is conventional spectroscopic practice to label the molecular eigenstates of a given J as F_1, F_2, and F_3 in order of increasing energy.[1,44,45] In the case (b) limit, where the spin–spin interaction is negligible compared to the rotational spacings, the wave functions are labeled according to the quantum number N, where $\mathbf{N}=\mathbf{J}-\mathbf{S}$ is the nuclear rotational angular momentum. Thus, N equals $J-1$, J, and $J+1$ for the F_1, F_2, and F_3 levels. The corresponding wave functions can be expressed in terms of the case (a) basis as[45,49]

$$|JMF_1\rangle=\sin\theta_J|JM\Omega=1,\epsilon=+1\rangle + \cos\theta_J|JM\Omega=0\rangle\,, \tag{18}$$

$$|JMF_2\rangle=|JM\Omega=1,\epsilon=-1\rangle\,, \tag{19}$$

$$|JMF_3\rangle=\cos\theta_J|JM\Omega=1,\epsilon=+1\rangle - \sin\theta_J|JM\Omega=0\rangle\,. \tag{20}$$

The mixing angle θ_J depends on J and the spectroscopic constants in the $^3\Sigma$ state and approaches $\pi/4$ in the high-J case (b) limit. Thus, in this limit the F_1 and F_3 levels are made up of equal mixtures of the $\Omega=0$ and $\Omega=1,\epsilon=+1$ states. We also see from Eq. (19) that the $\Omega=1,\epsilon=-1$ level is not mixed with either of the other two levels.

Using Eqs. (7), (8), (14), and (15), one can show that the expectation value for $\sigma_v(xz)$ when $M\cong 0$ is given by, for $i=1$ and 3,

$$\langle J,M=0,F_i|\sigma_v(xz)|J,M=0,F_i\rangle=\sin^2\theta_J+\cos^2\theta_J=+1\,, \tag{21}$$

while

$$\langle J,M=0,F_2|\sigma_v(xz)|J,M=0,F_2\rangle=-1\,. \tag{22}$$

Thus, we see that for high J, when the xz plane can be identified with the plane of rotation, the F_1 and F_3 levels are *symmetric* with respect to reflection of the electronic spatial *and* spin coordinates through this plane, while the F_2 levels are *antisymmetric*. Comparison of Eqs. (16) and (17) with Eqs. (21) and (22) shows that the reflection symmetry does not change between the case (a) and (b) limits.

In the case of a coplanar dissociation the plane of rotation of the NH fragment will be the same as the plane of rotation of the initial HN_3 molecule. Since the wave functions in the F_1 and F_3 spin-multiplet levels are symmetric with respect to reflection of the electronic coordinates in this plane of rotation, the discussion at the beginning of this section implies that only these two levels, and not the F_2 level, whose wave function is antisymmetric, should be produced in the ground state dissociation of HN_3. This is what has been found experimentally by Stephenson, Casassa, Foy, and King.[19,20] The reader should note that the reflection symmetry is with respect to the body-frame plane of rotation, so that this symmetry argument will apply irrespective of the rotational level of the HN_3 molecule, provided, of course that out-of-plane NN–NH torsional motion is insignificant at the transition state. One might expect that out-of-plane motion would be substantially reduced in the overtone pumping experiments of Foy *et al.*,[20] in which five and six quanta of the in-plane NH stretch were excited, as compared with the IRMPD experiments.[19] Consequently, as has been found experimentally,[20] the F_1/F_2 spin selectivity will be even more pronounced in the overtone pumping experiments. An additional experimental confirmation of our hypothesis of coplanar dissociation could be provided by the analysis of the correlation between the orientation of the velocity vector $\mathbf{v}$ and the rotational angular momentum $\mathbf{J}$ of the $NH(X\,^3\Sigma^-)$ fragment; coplanar dissociation would lead to $\mathbf{v}\perp\mathbf{J}$. Unfortunately, Stephenson and co-workers[19] were not able to extract this vector correlation information for the $NH(X\,^3\Sigma^-)$ channel.

We should point out that the reflection symmetry refers to the body-frame plane of rotation of the NH molecule. In the case of a coplanar dissociation the plane of rotation of the NH fragment will be the same as the plane of rotation of the initial HN_3 molecule.

V. Λ-DOUBLET SPECIFICITY IN THE DISSOCIATION OF HN_3 TO GIVE $NH(a\,^1\Delta)$ PRODUCTS

One can extend the symmetry argument used in the previous section to treat dissociation via the lowest energy singlet channel, leading to $NH(a\,^1\Delta)$ products. If the HN_3 molecule remains planar during this spin-allowed dissociation, the wave function of the NH fragment must also be symmetric with respect to reflection since the initial wave function is symmetric with respect to reflection in the plane of rotation and the wave function of the N_2 fragment is symmetric. As in Sec. IV, a proper analysis involves consideration of both the electronic and rotational wave functions of the NH fragment.

The wave function for a diatomic molecule in a $^1\Delta$ electronic states can be expressed in a definite parity case (a) basis as[24,44,48]

$$|JM\Lambda=2,e/f\rangle=2^{-1/2}[|JM\Omega=2\rangle|\Lambda=2\rangle + \epsilon|JM,\Omega=-2\rangle|\Lambda=-2\rangle]\,. \tag{23}$$

Since the total parity[50] of this wave function is $\epsilon(-1)^J$, the levels with $\epsilon=+1$ are labeled e and those with $\epsilon=-1$, f.[51] The analysis used in our previous investigation of the symmetry of Π electronic states,[2] can be extended easily to states of Δ symmetry. The symmetry with respect to reflection of the spatial coordinates of the electrons in a plane containing the molecular axis is the relevant measure of the symmetry of the wave function since the total electron spin S equals zero.

The analysis follows that of Sec. IV and our earlier papers.[2] The expectation value of σ_v is given by

$$\langle JM,\Lambda=2,e/f|\sigma_v(pq)|JM,\Lambda=2,e/f\rangle = \epsilon S_{2,-2}(J,M) \times\langle\Lambda'=2|\sigma_v(pq)|\Lambda=-2\rangle , \quad (24)$$

where $S_{2,-2}$ is defined by Eq. (11). As in Sec. IV we shall consider in detail only the $M\cong 0$ case, in which case we identify the plane of rotation with the xz plane.[2] The result of reflection of the spatial coordinates of the electrons on the electronic wave function is[50]

$$\sigma_v(xz)|\Lambda\rangle = (-1)^{\Lambda}|-\Lambda\rangle . \quad (25)$$

Furthermore, as demonstrated in Appendix B,

$$S_{2,-2}(J,0) = 1 . \quad (26)$$

Thus, we observe that the e Λ-doublet level is symmetric and consequently labeled $\Delta(A')$,[3] and the f Λ-doublet level, antisymmetric and labeled $\Delta(A'')$. Hence we predict that if the spin-allowed, singlet dissociation of HN_3 is dominated by a planar configuration, then the $NH(a\,^1\Delta)$ products will be formed predominantly in the e, or $\Delta(A')$, levels.

Experimentally,[19] the internal state distributions of NH products formed in the $a\,^1\Delta$ state are probed by laser induced fluorescence using the $c\,^1\Pi \leftarrow a\,^1\Delta$ band system.[54] The spectrum associated with a $^1\Pi \leftarrow {}^1\Delta$ transition consists of[1,54] P and R branch doublets, which corresponds to $f \leftarrow f$ and $e \leftarrow e$ transitions between the Λ-doublet levels of the lower and upper states, and Q branch doublets, which correspond to $e \leftarrow f$ and $f \leftarrow e$ transitions. The assignment of the NH $c\,^1\Pi \leftarrow a\,^1\Delta$ spectra using the modern e/f notation[51] has been discussed by Bernath and co-workers.[54]

Stephenson, Casassa, and King[19] do observe a preference for production of $NH(a^1\Delta)$ e levels, as predicted by our symmetry analysis, although here the symmetry selectivity is less strong than found for the triplet $[NH(X\,^3\Sigma^-)]$ channel. As discusssd at the end of Sec. IV, a coplanar dissociation would lead the a perpendicular orientation of the velocity **v** and angular momentum **J** vectors of the NH fragments. In their analysis of the $NH(a\,^1\Delta)$ fragments Stephenson, Casassa, and King[19] found a slight propensity for **v** *parallel* to **J**. Thus it may be that the observed $NH(a\,^1\Delta)$ products emanate from HN_3 molecules with a substantial degree of nonplanar motion, which would reduce the propensity toward production of $NH(a\,^1\Delta)$ in only e levels. This participation of nonplanar HN_3 geometries could arise from substantial torques in the singlet exit channel, beyond the point of singlet–triplet crossing. Alternatively, since more internal energy is required to reach the higher energy singlet channel, under IRMPD conditions, the more highly excited HN_3 molecules which lead to $NH(a\,^1\Delta)$ could certainly be expected to have a greater degree of nonplanar torsional excitation than those molecules which decompose to the lower energy $NH(X\,^3\Sigma^-)$ channel.

VI. DISCUSSION

This article has been devoted to an investigation of the energetics and mechanism of the dissociation of ground state $HN_3(\tilde{X}\,^1A')$ into ground state $N_2(X\,^1\Sigma_g^+) + NH(X\,^3\Sigma^-)$ products. This process, which can be induced by multiphoton infrared pumping, occurs through a crossing between the lowest energy singlet potential energy surface, which correlates asymptotically with electronically excited NH products ($a\,^1\Delta$), and the lowest triplet surface. By means of *ab initio* CASSCF and MCSCF-CI calculations we have located the geometry corresponding to the minimum singlet–triplet crossing which defines the transition state for the ground state dissociation, as well as the height of this transition state above the HN_3 minimum. Without including any zero-point corrections, we observe that our estimate of this activation energy ($\sim 12\,500\ cm^{-1}$) agrees well with the value $E_a \cong 36$ kcal/mol $= 12\,700\ cm^{-1}$ estimated by Kajimoto *et al.*[55] from thermal dissociation studies in a shock tube.

The geometry of the singlet–triplet crossing corresponds to an approximately linear N_3 backbone with a perpendicular NH bond. The interior N–N distance is ~ 3.5 bohr. Since the N–N and N–H bonds are perpendicular at this transition state, there will be no torques tending to twist the system out of a planar geometry. Additional CASSCF calculations were used to explore the topology of the surface in the region of the singlet–triplet crossing. Since the polar orientation of the NH bond with respect to the N_2 bond is virtually unchanged in the region of the singlet–triplet crossing and since in the exit channel the $^3A''$ surface is steeply repulsive in the NN–NH separation coordinate but is not strongly dependent on the NN–NH polar angle, we expect that energy release will be primarily into the relative translational motion of the two fragments rather into than into rotation. Furthermore, since the terminal N–N and the N–H distances at the point of singlet–triplet crossing are very close to the value in the ground electronic states of the N_2 and NH molecules, we expect not to see any significant degree of vibrational excitation in the N_2 and NH dissociation products.

The HN_3 wave function in the region of this singlet–triplet crossing can be considered an equal admixture of $N_2(X)\cdot NH(a\,^1\Delta)$ and $N_2(X)\cdot NH(b\,^1\Sigma^+)$. Thus, although there is no spin–orbit coupling between a $^1\Delta$ and a $^3\Sigma^-$ state, the singlet–triplet coupling leading to dissociation of HN_3 can occur by means of the $NH(b\,^1\Sigma^+)$ component in the singlet HN_3 wave function, since a $^1\Sigma^+$ and a $^3\Sigma^-$ state are coupled by the $l_z s_z$ term in the spin–orbit Hamiltonian.

The ground state HN_3 wave function is symmetric with respect to reflection of the spatial and spin components of all the electrons in the plane of the molecule. Thus, since the $l_z s_z$ term in the spin–orbit Hamiltonian is also symmetric, and since the NH fragment must rotate in the plane of the initial HN_3 molecule if the dissociation is planar, NH products can be formed only in states in which the wave function (electronic + rotational) is also symmetric with respect to reflection of the spatial and spin coordinates of all the electrons in the plane of rotation of the NH molecule. We then showed that the wavefunctions in the F_1 and F_3 levels of a molecule in a $^3\Sigma^-$ electronic state were symmetric, and in the F_2 levels, antisymmetric with respect to this operation. Thus one would expect population predominantly in the F_1 and F_3 levels. Similarly, in the $NH(a\,^1\Delta)$ products formed in the spin-allowed singlet channel, one would expect population predominantly in the e $[\Delta(A')]$ Λ-doublet level, whose wave function is symmetric with respect to reflection of the

spatial coordinates of the electrons in the plane of rotation of the NH molecule.

This spin[19,20] and Λ-doublet[19] selection has been found experimentally by Stephenson, Casassa, Foy, and King, although some population was seen in the antisymmetric F_2 levels in the $X\,^3\Sigma^-$ state and in the antisymmetric $f[\Delta(A'')]$ Λ-doublet levels of the $a\,^1\Delta$ state. This is probably a consequence of slight dihedral torques, since in the transition state (Fig. 2) the N–N and N–H bonds are not quite perpendicular. Alternatively, if the infrared pumping process used by Stephenson, Casassa, and King[19] leads to excitation of out-of-plane wagging vibrations, then some deviation from coplanarity will be present at the transition state.

As mentioned in the Introduction, a similar deviation from nonstatistical spin multiplet populations have been seen in the uv photolysis of SO_2 to yield $SO(X\,^3\Sigma^-) + O(^3P)$. This process is also thought to involve a singlet–triplet crossing in the exit channel. In this case the analysis may be more complex, since both symmetric and antisymmetric wave functions are possible for the various multiplet levels of the $O(^3P)$ fragment, in contrast to the case of HN_3, where the wave function of the N_2 fragment is always symmetric. Nevertheless, we believe that an analysis similar to that presented here will be of great use in the interpretation of anomalous spin state populations in the photodissociation of both SO_2[25] and O_3.[56,57]

For the latter molecule, an even–odd alternation has been found[56] in the rotational populations of $^{16}O_2$, but not for $^{16}O^{18}O$, fragments in the $a\,^1\Delta_g$ state formed from the near UV photodissociation of ozone in the Hartley bands. This has been interpreted as arising from a selective depletion of only odd-J rotational levels of $^{16}O_2(a\,^1\Delta_g)$ by a curve crossing to form $^{16}O_2(X\,^3\Sigma_g^-)$ products. The conservation of nuclear permutation symmetry is responsible for this selectivity. This curve crossing process is entirely analogous to that investigated theoretically here for HN_3 and would be expected to conserve reflection symmetry and to yield nonstatistical spin multiplet populations in the $^{16}O_2(X\,^3\Sigma_g^-)$ products. At present the CARS studies by Valentini and coworkers[56,57] can resolve only the rotational levels, but not individual spin levels, in O_2.

We would also expect to observe a spin-state selectivity identical to that found for HN_3 in the ground state dissociation of the isoelectronic HNCO molecule, where the CO fragment is, like N_2, in a symmetric $^1\Sigma^+$ state. Only UV photolysis of HNCO has been studied experimentally,[58,59] in which case, similarly to the UV photolysis of HN_3,[21–23] just the singlet channel is observed, namely,

$$HNCO \rightarrow CO(X\,^1\Sigma^+) + NH(a\,^1\Delta)\,. \tag{27}$$

Finally, one might also anticipate spin selectivity in the ground state dissociation of ketene (H_2CCO) to yield spin-forbidden triplet methylene products:

$$H_2CCO \rightarrow CH_2(\tilde{X}\,^3\Sigma_g^-) + CO(X\,^1\Sigma^+)\,, \tag{28}$$

and in the photodissociation of the fluorine azide (FN_3) or diazomethane (CH_2N_2) molecules, namely

$$FN_3 \rightarrow N_2(X\,^1\Sigma_g^+) + NF(X\,^3\Sigma^-, a\,^1\Delta) \tag{29}$$

and

$$H_2CN_2 \rightarrow CH_2(\tilde{X}\,^3\Sigma_g^-) + N_2(X\,^1\Sigma_g^+)\,. \tag{30}$$

An *ab inito* study of the energetics of the dissociation of FN_3 has been already reported by Michels.[60]

Other important questions remain concerning the dissociation of HN_3, notably the topology of the surfaces leading to production of lowest two singlet channels [$NH(a\,^1\Delta)$ and $NH(b\,^1\Sigma^+)$]. It appears from the experimental work of Stephenson, Casassa, and King[19] that there may exist a barrier in the lowest singlet channel. In our MCSCF-CI calculations the energy of the lowest singlet state was found to increase continuously with increasing values of the NH–NH distance up to the maximum value investigated (4.5 bohr). Some CASSCF calculations with the 10/6/1–6/2 basis, carried out for larger distances, suggested a barrier on the singlet surface at large (5–6 bohr) NN–NH separations. Obviously, further calculations need to be done to pin down fully this feature. Ultimately one would like to use the HN_3 potential energy surfaces determined here to calculate actual dissociation rates and product state distributions, possibly by trajectory surface–hopping methods.[61–63]

ACKNOWLEDGMENTS

The research described here was partially supported by the U. S. Air Force Office of Scientific Research under Grant 87-NC-119. Most of the *ab initio* calculations were carried out at the San Diego Supercomputer Center, under an allocation of time to M.H.A. in connection with NSF grant CHE87-05828. The participation of H.J.W. was made possible by the Deutsche Forschungsgemeinschaft and by the German Fonds der Chemischen Industrie. M.H.A. is grateful to David King and John Stevenson for several discussions about their experimental work, to Brigitte Pouilly for her insight into the subtleties of spin–orbit coupling, and to Peter Bernath for helpful comments about the spectroscopic constants of the low-lying states of NH.

APPENDIX A: REFLECTION SYMMETRY OF SPIN 1/2 AND SPIN 1 FUNCTIONS

For clarity and completeness we derive here explicitly the reflection symmetry of the spin 1/2 functions in a Hund's case (a) limit, where the spin is assumed to be quantized along the molecule-frame z axis. Much of this discussion follows that of Judd,[64] and the important results have been given earlier by Hougen[44] and Røggen.[65] The spin functions will be denoted $|1/2\rangle$ and $|-1/2\rangle$. Let us consider first reflection in the xz plane. This operation can be achieved by an inversion followed by a rotation of π around the new y axis.[64] In other words

$$\sigma_v(xz) = D(0,\pi,0)I\,, \tag{A1}$$

where I is the inversion operator and $D(\alpha,\beta,\gamma)$ is the operator for rotation of the coordinate system through the Euler angles α, β, γ. Note that in contrast to Sec. IV, here we are using the so-called "passive" convention in which the coordinate system, rather than the figure, is rotated.[50,66] Since the spin 1/2 functions are taken to be symmetric with respect to inversion, Eq. (A1) implies

$$\sigma_v(xz)|1/2\rangle = d^{1/2}_{1/2,1/2}(\pi)|1/2\rangle + d^{1/2}_{-1/2,1/2}(\pi)|-1/2\rangle , \quad \text{(A2)}$$

and similarly for $\sigma_v(xz)|-1/2\rangle$. Introduction of the explicit form of the $d^{1/2}_{m,n}(\pi)$ reduced matrix elements[52] leads to the following equations:

$$\sigma_v(xz)|1/2\rangle = |-1/2\rangle \quad \text{(A3a)}$$

and

$$\sigma_v(xz)|-1/2\rangle = -|1/2\rangle , \quad \text{(A3a)}$$

which can be generalized as

$$\sigma_v(xz)|S\Sigma\rangle = (-1)^{S-\Sigma}|S-\Sigma\rangle . \quad \text{(A4)}$$

The wave function for a state with total spin 1 can be constructed out of Slater determinants containing two half-filled spin orbitals. Neglecting all closed-shell orbitals, we can represent the three $S=1$ wave functions as

$$|S,\Sigma=1\rangle = |ab|, \quad \text{(A5)}$$

$$|S,\Sigma=0\rangle = 2^{-1/2}[|a\bar{b}| + |\bar{a}b|], \quad \text{(A6)}$$

and

$$|S,\Sigma=-1\rangle = |\bar{a}\bar{b}| . \quad \text{(A7)}$$

Here a and b designate two molecular orbitals. As is usual, a superscript bar indicates that the projection of the spin along the molecule-frame z axis is $\Sigma = -1/2$; the absence of a bar indicates a projection quantum number of $+1/2$. Obviously the reflection operator for both electrons is the product of the reflection operator for the individual electrons. It is easy to show from Eq. (A3) that the relation $\sigma_v(xz)|S\Sigma\rangle = (-1)^{S-\Sigma}|S-\Sigma\rangle$ [Eq. (A4)] also applies to wave functions of total spin 1. A similar proof applies to functions of higher multiplicity.

We turn now to reflection in the yz plane. This can be achieved by a rotation of the coordinate system through the Euler angles $(0,\pi,-\pi)$ followed by an inversion. Thus Eq. (A2) is replaced by

$$\sigma_v(yz)|1/2\rangle = D^{1/2}_{1/2,1/2}(0,\pi,-\pi)|1/2\rangle + D^{1/2}_{-1/2,1/2}(0,\pi,-\pi)|-1/2\rangle , \quad \text{(A8)}$$

and similarly for $\sigma_v(yz)|-1/2\rangle$. In this case Eq. (A3) becomes replaced by

$$\sigma_v(yz)|1/2\rangle = i|-1/2\rangle \quad \text{(A9a)}$$

and

$$\sigma_v(yz)|-1/2\rangle = i|1/2\rangle , \quad \text{(A9b)}$$

which can be generalized as

$$\sigma_v(yz)|S\Sigma\rangle = (-1)^S|S-\Sigma\rangle . \quad \text{(A10)}$$

In the case of wave functions of triplet multiplicity, an expansion in Slater determinants, similar to that done above, can be used to show that Eq. (A10) remains valid for all values of S and Σ.

APPENDIX B: EVALUATION OF THE INTEGRAL $S_{2,-2}(J,0)$

We need to evaluate

$$S_{2,-2}(J,0) = \left[\frac{2J+1}{4\pi}\right]\int_0^{2\pi} d\alpha \int_0^{\pi} \sin\beta D^J_{0,2}(\alpha\beta 0) \times D^{J*}_{0,-2}(\alpha\beta 0)d\beta . \quad \text{(B1)}$$

We can substitute to give an integral over reduced rotation matrix elements:

$$S_{2,-2}(J,0) = \left(J+\frac{1}{2}\right)\int_0^{\pi} \sin\beta d^J_{0,2}(\beta) d^J_{0,-2}(\beta)d\beta . \quad \text{(B2)}$$

But[52]

$$d^J_{0,-2}(\beta) = d^J_{2,0}(\beta) \quad \text{(B3)}$$

and

$$d^J_{0,2}(\beta) = d^J_{2,0}(\beta) , \quad \text{(B4)}$$

so that

$$S_{2,-2}(J,0) = \left(J+\frac{1}{2}\right)\int_0^{\pi} \sin\beta \left[d^J_{2,0}(\beta)\right]^2 d\beta . \quad \text{(B5)}$$

We can express the reduced rotation matrix element in the above equation as follows:

$$d^J_{2,0}(\beta) = (-1)^2\left[\frac{(J-2)!}{(J+2)!}\right]^{1/2} P^2_J(\cos\beta) . \quad \text{(B6)}$$

Thus $S_{2,-2}(J,0)$ becomes

$$S_{2,-2}(J,0) = \frac{(2J+1)(J-2)!}{2(J+2)!} \times \int_0^{\pi} \sin\beta \left[P^2_J(\cos\beta)\right]^2 d\beta . \quad \text{(B7)}$$

But the integral in Eq. (B7) equals[67]

$$\int_0^{\pi} \sin\beta \left[P^2_J(\cos\beta)\right]^2 d\beta = \frac{2(J+2)!}{(2J+1)(J-2)!} . \quad \text{(B8)}$$

Hence, we find

$$S_{2,-2}(J,0) = +1 . \quad \text{(B9)}$$

[1] G. Herzberg, *Molecular Spectra and Molecular Structure. I. Spectra of Diatomic Molecules* (Van Nostrand, Princeton, 1950).
[2] M. H. Alexander and P. J. Dagdigian, J. Chem. Phys. **80**, 4325 (1984); B. Pouilly, P. J. Dagdigian, and M. H. Alexander, *ibid.* **87**, 7118 (1987).
[3] M. H. Alexander, P. Andresen, R. Bacis, R. Bersohn, F. J. Comes, P. J. Dagdigian, R. N. Dixon, R. W. Field, G. W. Flynn, K.-H. Gericke, E. R. Grant, B. J. Howard, J. R. Huber, D. S. King, J. L. Kinsey, K. Kleinermanns, K. Kuchitsu, A. C. Luntz, A. J. McCaffery, B. Pouilly, H. Reisler, S. Rosenwaks, E. W. Rothe, M. Shapiro, J. P. Simons, R. Vasudev, J. R. Wiesenfeld, C. Wittig, and R. N. Zare, J. Chem. Phys. (in press).
[4] R. Vasudev, R. N. Zare, and R. N. Dixon, J. Chem. Phys. **80**, 4863 (1984).
[5] M. P. Docker, A. Hodgson, and J. P. Simons, Faraday Discuss. Chem. Soc. **82**, 25 (1986); J. P. Simons, J. Phys. Chem. **91**, 5378 (1987).
[6] P. Andresen, G. S. Ondrey, B. Titze, and E. W. Rothe, J. Chem. Phys. **80**, 2548 (1984); D. Häusler, P. Andresen, and R. Schinke, *ibid.* **87**, 3949 (1987).
[7] K.-H. Gericke, S. Klee, F. J. Comes, and R. N. Dixon, J. Chem. Phys. **85**, 4463 (1986); A. U. Grunewald, K.-H. Gericke, and F. J. Comes, *ibid.* **87**, 5709 (1987).
[8] F. Lahmani, C. Lardeux, and D. Solgadi, Chem. Phys. Lett. **129**, 24 (1986).
[9] D. Schwartz-Lavi, I. Bar, and S. Rosenwaks, Chem. Phys. Lett. **128**, 123

(1986); R. Lavi, I. Bar, and S. Rosenwaks, J. Chem. Phys. **86**, 1639 (1987); R. Lavi, D. Schwartz-Lavi, I. Bar, and S. Rosenwaks, J. Phys. Chem. **91**, 5398 (1987).
[10]M. Dubs, U. Brühlmann, and J. R. Huber, J. Chem. Phys. **84**, 3106 (1986); U. Brühlmann, M. Dubs, and J. R. Huber, *ibid.* **86**, 1249 (1987); U. Brühlmann, and J. R. Huber, Chem. Phys. Lett. **143**, 199 (1988).
[11]F. Alberti and A. E. Douglas, Chem. Phys. **34**, 399 (1978).
[12]A. M. Quinton and J. P. Simons, Chem. Phys. Lett. **81**, 214 (1981).
[13]L. Bigio and E. R. Grant, J. Phys. Chem. **89**, 5855 (1985); J. Chem. Phys. **87**, 360, 5589 (1987).
[14]D. S. King and J. C. Stephenson, J. Chem. Phys. **82**, 2236 (1985); M. P. Casassa, J. C. Stephenson, and D. S. King, Faraday Discuss. Chem. Soc. **82**, 251 (1986).
[15]M. Noble, C. X. W. Qian, H. Reisler, and C. Wittig, J. Chem. Phys. **85**, 5763 (1986).
[16]M. R. S. McCoustra and J. Pfab, Chem. Phys. Lett. **137**, 355 (1987).
[17]F. Shokoohi, S. Hay, and C. Wittig, Chem. Phys. Lett. **110**, 1 (1984); I. Nadler, D. Mahgerefteh, H. Reisler, and C. Wittig, J. Chem. Phys. **82**, 3885 (1985).
[18]H. Joswig, M. A. O'Halloran, R. N. Zare, and M. S. Child, Faraday Discuss. Chem. Soc. **82**, 83 (1986).
[19]J. C. Stephenson, M. P. Casassa, and D. S. King, J. Chem. Phys. **89**, 1378 (1988).
[20]B. R. Foy, M. P. Casassa, J. C. Stephenson, and D. S. King, J. Chem. Phys. **89**, 608 (1988)
[21]J. R. McDonald, R. G. Miller, and A. P. Baronavski, Chem. Phys. Lett. **51**, 119 (1978); A. P. Baronavski, R. G. Miller, and J. R. McDonald, Chem. Phys. **30**, 119 (1978).
[22]L. G. Piper, R. H. Krech, and R. L. Taylor, J. Chem. Phys. **73**, 791 (1980).
[23]F. Rohrer and F. Stuhl, Chem. Phys. Lett. **111**, 234 (1984).
[24]H. Lefebvre-Brion and R. W. Field, *Perturbations in the Spectra of Diatomic Molecules* (Academic, New York, 1986).
[25]H. Kanamori, J. E. Butler, K. Kawaguchi, C. Yamada, and E. Hirota, J. Chem. Phys. **83**, 611 (1985).
[26]B. P. Winnewiser, J. Mol. Spectrosc. **82**, 220 (1980).
[27]S. W. Harrison, C. R. Fischer, and P. J. Kemmey, Chem. Phys. Lett. **36**, 229 (1975).
[28]J. Lieven, J. Breulet, and G. Verhaegen, Theor. Chim. Acta **52**, 75 (1979).
[29]C. E. Sjøgren and C. J. Nielsen, J. Mol. Struct. **XX**, 285 (1986).
[30]D. J. deFrees, G. H. Loew, and A. D. McLean, Astrophys. J. **254**, 405 (1982).
[31]H.-J. Werner and W. Meyer, J. Chem. Phys. **73**, 2342 (1980), and references therein.
[32]H.-J. Werner, Adv. Chem. Phys. **49**, 1 (1987), and references therein.
[33]H.-J. Werner and W. Meyer, J. Chem. Phys. **74**, 5794 (1981).
[34]H.-J. Werner and P. J. Knowles, J. Chem. Phys. **82**, 5053 (1985).
[35]P. J. Knowles and H.-J. Werner, Chem. Phys. Lett. **115**, 259 (1985).
[36]H.-J. Werner and E. A. Reinsch, J. Chem. Phys. **76**, 3144 (1982).
[37]H.-J. Werner and E. A. Reinsch, in *Advanced Theories and Computational Approaches to the Electronic Structure of Molecules*, edited by C. E. Dykstra (Reidel, Dordrecht, 1984), p. 79.
[38]H.-J. Werner and P. J. Knowles, J. Chem. Phys. (submitted).
[39]S. Huzinaga, J. Chem. Phys. **42**, 1293 (1965); Technical Report, Approximate Atomic Functions, Department of Chemistry, University of Alberta (1965).
[40]S. R. Langhoff and E. R. Davidson, Int. J. Quantum Chem. **8**, 61 (1974).
[41]W. Meyer and P. Rosmus, J. Chem. Phys. **63**, 2356 (1975).
[42]C. M. Marian and R. Klotz, Chem. Phys. **95**, 213 (1985).
[43]K. P. Huber and G. Herzberg, *Molecular Spectra and Molecular Structure. IV. Constants of Diatomic Molecules* (Van Nostrand Reinhold, New York, 1979).
[44]J. T. Hougen, Natl. Bur. Stand. (U.S.) Monogr. **115** (1970).
[45]J. B. Tatum and J. K. G. Watson, Can. J. Phys. **49**, 2693 (1971).
[46]K. Kayama and J. C. Baird, J. Chem. Phys. **46**, 2604 (1967).
[47]See J. O. Jensen and D. R. Yarkony, Chem. Phys. Lett. **141**, 391 (1987).
[48]R. N. Zare, A. L. Schmeltekopf, W. J. Harrop, and D. L. Albritton, J. Mol. Spectrosc. **46**, 371 (1973).
[49]M. H. Alexander and P. J. Dagdigian, J. Chem. Phys. **79**, 302 (1983).
[50]M. Larsson, Phys. Scr. **23**, 835 (1981).
[51]J. M. Brown, J. T. Hougen, K. P. Huber, J. W. C. Johns, I. Kopp, H. Lefebvre-Brion, A. J. Merer, D. A. Ramsay, J. Rostas, and R. N. Zare, J. Mol. Spectrosc. **55**, 500 (1975).
[52]D. M. Brink and G. R. Satchler, *Angular Momentum*, 2nd ed. (Clarendon, Oxford, 1968).
[53]S. Green and R. N. Zare, Chem. Phys. **7**, 62 (1975).
[54]R. S. Ram and P. F. Bernath, J. Opt. Soc. Am. B **3**, 1170 (1986).
[55]O. Kajimoto, T. Yamamoto, and T. Fueno, J. Phys. Chem. **83**, 429 (1979).
[56]J. J. Valentini, D. P. Gerrity, D. L. Phillips, J.-C. Nieh, and K. D. Tabor, J. Chem. Phys. **86**, 6745 (1987); J. J. Valentini, *ibid.* **86**, 6757 (1987).
[57]H. B. Levene, J.-C. Nieh, and J. J. Valentini, J. Chem. Phys. **87**, 2583 (1987).
[58]W. S. Drozdoski, A. P. Baronavski, and J. R. McDonald, Chem. Phys. Lett. **64**, 421 (1979).
[59]T. A. Spiglanin, R. A. Perry, and D. W. Chandler, J. Phys. Chem. **90**, 6184 (1986); T. A. Spiglanin and D. W. Chandler, J. Chem. Phys. **87**, 1577 (1987).
[60]H. Michels, Proceedings of First Topical Conference on High Energy Density Materials, June, 1987.
[61]J. C. Tully, in *Modern Theoretical Chemistry*, edited by W. H. Miller (Plenum, New York, 1976).
[62]B. C. Garrett and D. G. Truhlar, in *Theoretical Chemistry: Advances and Perspectives*, edited by D. Henderson (Academic, New York, 1981).
[63]D. G. Truhlar and J. T. Muckerman, in *Atom-Molecular Collision Theory: A Guide for the Experimentalist*, edited by R. B. Bernstein (Plenum, New York, 1979), p. 505.
[64]B. R. Judd, *Angular Momentum Theory for Diatomic Molecules* (Academic, New York, 1975).
[65]I. Röeggen, Theor. Chim. Acta **21**, 398 (1971).
[66]A. R. Edmonds, *Angular Momentum in Quantum Mechanics* (Princeton University, Princeton, 1960).
[67]L. D. Landau and E. M. Lifshitz, *Quantum Mechanics: Non-Relativistic Theory*, 2nd ed. (Pergamon, Oxford, 1965), p. 600.